

R. F. Silva · M. De Francesco · L. Giorgi
M. C. Campa · F. Cardellini · A. Pozio

Highly stable Pt–Ru/C as an anode catalyst for use in polymer electrolyte fuel cells

Received: 29 July 2003 / Accepted: 14 November 2003 / Published online: 24 January 2004
© Springer-Verlag 2004

Abstract A new method for preparing highly stable Pt–Ru/C catalysts at low temperature is reported. Pt–Ru supported on high surface carbon was prepared from $\text{Pt}(\text{NH}_3)_4\text{Cl}_2$, $\text{RuNO}(\text{NO}_3)_x(\text{OH})_y$ and borohydride as a reducing agent. Simultaneous reduction of both metals was done by heat treatment and small and homogeneously dispersed catalyst particles were obtained with increased stability, as observed from solubility tests. Catalysis, XRD and TG data gave clear evidence of the different chemical states between the material produced and the commercially available sample. The electrochemical measurements showed that the novel catalysts have a performance similar to that of E-Tek samples.

Keywords Catalysts · PEFCs · DAFCs · Hydrogen oxidation · Pt alloy

Introduction

Polymer electrolyte fuel cells (PEFCs) and direct alcohol fuel cells (DAFCs) with high power density performance at low temperature (70–90 °C) are promising energy sources for electric vehicles and portable devices. In PEFCs, the anode gas stream is hydrogen rich, containing also CO_2 and CO produced by reforming or partial oxidation of hydrocarbons. In DAFCs, a direct oxidation of an alcohol (ethanol or methanol) to CO_2 occurs with the production of derived carbonyl species, mainly CO. In the presence of CO, the Pt/C anode

catalyst is subjected to poisoning even at very low concentrations (10 ppm). A possible solution for this problem consists in the use of CO tolerant catalysts formed by alloying Pt with a second transition metal (e.g. Ru, Mo) [1, 2, 3, 4]. So far, the best CO tolerant catalyst appears to be the Pt–Ru alloy, which is more active than pure Pt in $\text{H}_2 + 100$ ppm CO anode gas stream. Carbon supported Pt–Ru catalysts can be prepared using several processes [5, 6, 7, 8]. The electrocatalytic activity of Pt–Ru/C is intimately related to the preparation process. Luna et al. [5] obtained Pt–Ru/C catalysts with best performance by using Watanabe's modified method, which consists of providing the sample with a thermal treatment at 300 °C in an H_2 atmosphere after the original procedure proposed by Watanabe et al. [8]. The performance of their catalysts is similar to that of commercial E-Tek Pt–Ru/C samples in pure hydrogen. In contrast, different preparation methods using other reduction agents such as formic acid or borohydride furnished worse results than those of the E-Tek samples [5]. However, the commercially available E-Tek 50:50 Pt–Ru/C catalyst (20% in weight of catalyst) has been shown to be poorly stable in ethanol and methanol at room temperature and its solubility is enhanced by increasing temperature or by using ultrasonic treatment, as predicted by many authors [5, 6, 7, 9, 10, 11], thus forming a homogeneous ink. An improvement of catalyst synthesis is needed to eliminate this problem in order to control the exact atomic ratio and ruthenium loading in the electrode, especially in DAFCs where ruthenium can be easily dissolved in ethanol or methanol and is thus lost during the cell lifetime. In addition, ionic ruthenium can diffuse into the polymeric membrane, linking to the sulfonic acid groups and consequently increasing the ohmic resistance [12, 13].

A new proprietary method for preparing stable, high surface Pt–Ru/C catalysts at low temperatures and in short times has been employed. Unlike Watanabe's modified method [5], the present route does not make use of thermal treatment in a hydrogen atmosphere and gives rise to catalysts with well-defined atomic ratios capable

R. F. Silva · M. D. Francesco · L. Giorgi
F. Cardellini · A. Pozio (✉)
C.R. Casaccia, ENEA,
Via Anguillarese 301,
00060 S. Maria di Galeria (Rome), Italy
E-mail: alfonso.pozio@casaccia.enea.it
Fax: +39-06-30486357

M. C. Campa
University of Rome,
P. le A. Moro 5,
00185 Rome, Italy

of performing similarly to commercial ones. The method results in lower cost than the traditional ones and appears to be easily scaled up to manufacturing levels.

In this paper the description of the method is presented as well as the characterisation of the catalyst produced and its comparison with commercial E-Tek.

Experimental

Pt–Ru/C catalyst preparation

Carbon black powder (Vulcan XC-72, Cabot International) with a specific surface area (BET) of $250 \text{ m}^2 \text{ g}^{-1}$ was used as a support for the catalyst. All the samples contained 20 wt.% of catalyst supported on carbon. The proprietary method for preparing the 50:50-at.% Pt–Ru/C catalyst has already been described in the literature [14]. Briefly, a 300-ml slurry composed by carbon black powder, $\text{Pt}(\text{NH}_3)_4\text{Cl}_2$, $\text{RuNO}(\text{NO}_3)_x(\text{OH})_y$ and 2-M NaOH solution was prepared. The ink was stirred at 90°C for 30 min and then cooled. A 0.5-M solution of sodium borohydride was added to the ink and the bath was heated to boiling temperature. The mixtures were cooled, dried and washed repeatedly with distilled water and finally the catalyst powders were heated overnight at 110°C in an air oven. Commercially available 50:50-at.% Pt–Ru/C catalyst supported on Vulcan XC-72 carbon black was purchased from E-Tek Inc. and used as a reference.

Electrode preparation

Three-layer (substrate/diffusive layer/catalyst layer) gas diffusion electrodes (GDEs) were prepared using Toray TGPH090 carbon paper as substrate. As already described in our previous work [11], the diffusive layer (DL) was prepared with a weight composition of 80 wt.% carbon, 20 wt.% PTFE and a loading of about 2 and 0.5 mg cm^{-2} , respectively. The catalyst layer (CL) was prepared by mixing and ultrasonically about 0.1 g of Pt–Ru/C powder and 3–4 ml of isopropanol in a glass vial at 40°C for 14 min. A volume of 1–2 ml of the formed ink was spread with a micropipette on the surface of the pre-weighed “CP + DL” disk and air-dried at 70°C for about 30 min to eliminate the solvent and to obtain a thin active layer. The GDE was weighed again and the Pt–Ru loading was calculated for each sample. A platinum loading of 2.1 mg cm^{-2} was achieved for all the electrodes. Commercially available 5 wt.% Nafion solution (DuPont) was carefully spread on the catalyst layer and air-dried at room temperature to protect it and avoid the loss of catalyst into the electrolyte [15].

Electrode preparation for full-cell measurements

Both the 20-wt.% Pt–Ru/C catalyst and the commercially available 40-wt.% Pt/C supported on Vulcan XC-72 carbon black were purchased from E-Tek Inc. Three-layer gas diffusion anode and cathode (106 cm^2) were prepared, as described in detail previously [11, 16]. Briefly, an ethanolic ink containing the ENEA or E-Tek catalyst and polytetrafluoroethylene (PTFE) was sprayed on Toray TGPH090 carbon paper. The weight composition of the diffusion layer was 85 wt.% carbon and 15 wt.% PTFE, with a carbon loading of 2.87 mg cm^{-2} and 1.68 mg cm^{-2} on the anode and cathode, respectively. The catalyst layer was prepared by mixing appropriate amounts of the carbon supported catalyst (67 wt.%) and 5 wt.% Nafion solution (33 wt.%). The cathode Pt loading and the anode Pt–Ru loading were kept constant at 0.94 mg cm^{-2} and 0.47 mg cm^{-2} , respectively. Nafion 112 membrane (DuPont) was used after purification treatment and the membrane electrode assemblies (MEAs) were formed by hot pressing the electrodes (106 cm^2) onto the membrane, as described elsewhere [11, 16].

Membrane electrode gasket assembly (MEGA) technology [16] was used and a well-defined shape compatible with the cell hardware was achieved. The end plates were aluminium anticorrosional 100 ($185 \text{ mm} \times 185 \text{ mm} \times 11 \text{ mm}$) purchased from Alusuisse. Graphite flow field plates were assembled with a typical parallel channel configuration using commercially available BMA5 graphite produced by SGL Carbon Group (Germany).

Physical chemical characterisation

X-ray diffractograms (XRD) were registered with a Philips diffractometer operating in the Bragg–Brentano parafocusing geometry. A Cu K_α ($\lambda = 1.5418 \text{ \AA}$) radiation source was used together with a graphite monochromator on the diffracted beam. A Philips mod. PW1729 high tension generator was operated at 40 kV and 30 mA in the step scan mode with a 0.05 step, acquisition time 36 s per step and in the 2θ range 15° – 90° .

Thermogravimetric (TG) analysis of the powder samples was carried out in a DuPont 2000 Thermal Analysis System with 1600 DTA and 951 TGA modules. TG measurements were run in dynamic air or nitrogen streams of 100 ml min^{-1} at a heating rate of 5°C min^{-1} in the range 25 – 300°C . About 15-mg samples were used and α -alumina powder was kept as the standard material.

To control the ruthenium loss after the ultrasonic treatment in the ENEA and E-Tek Pt–Ru/C catalysts, the following procedure was used: 30 mg of catalyst powder was dissolved in 10 ml of ethanol and the ink formed was ultrasonically blended at 25°C for 14 min and then left overnight. The sample was filtered and divided into two parts to detect the presence of Pt and Ru [14, 17, 18]. A method for controlling the ruthenium loss in ethanol and methanol without ultrasonic treatment was also used by leaving 30 mg of the catalyst powder in 10 ml of the two alcohols at 25°C for 11 days and at 65°C for 1 h.

Catalysis experiments

The catalytic activity was measured in a conventional flow apparatus at atmospheric pressure [19]. The apparatus included a feeding section where the three-gas streams (He, 10% O_2 in He, and 3% CO in He, high purity purchased from Rivoira) were regulated by means of independent mass flow controller-meters (MKS mod. 1259, driven by a four-channel unit MKS mod. 247 c) and mixed in a glass ampoule before entering the reactor. The reactor was made of silica with an internal sintered frit of about 12 mm diameter supporting the catalysts. The reactor was vertically positioned in an electric heater, with a thermocouple touching the external wall of the reactor at the middle of the catalyst bed. A commercial device was used to regulate temperature. A reactor by-pass was provided by a four-way valve. Reactants and products were analysed by gas chromatography using a Varian Quad Micro-GC CP-2003 equipped with two columns: (i) 10-m Molsieve 5A BF for detecting O_2 and CO, and (ii) 10-m Poraplot Q for detecting CO_2 . All experiments yielded satisfactory carbon balance.

A fresh portion of catalyst (0.2 g) was purged in flowing He at room temperature for 30 min, heated from room temperature to 623 K in a flow of 3% CO in He mixture for 1 h and then held at 623 K for 2 h. After purging with He at 623 K for 1 h, the reactor was by-passed and the temperature adjusted to the desired value. Catalysis experiments were run using stoichiometric mixtures of CO (0.4%) and O_2 (0.2%) with He as balance. After stabilisation of the reactants, the valve was switched and the reaction mixture was allowed to flow onto the catalyst. The reaction temperature or mixture composition was changed without intermediate activation treatment. The total flow rate (F_t) was generally maintained at $50 \text{ ml (STP) min}^{-1}$. The reaction rates (R_g) calculated from the CO_2 produced or CO consumed were expressed as molecules of CO converted to CO_2 per second per gram of metal. The reaction rates were evaluated from experiments yielding conversion of less than 50%.

Electrochemical characterisation of the electrodes

Galvanostatic polarisation and electrochemical impedance spectroscopy (EIS) measurements were carried out in a conventional three-electrode cell (anode/counter electrode/reference electrode) containing a 1-M H_2SO_4 solution at 25 °C [11, 18]. The gas diffusion electrode was placed inside a Teflon holder provided with a platinum-ring current collector and gas back-feeding. A stream of 16 ml min^{-1} of H_2 or $\text{H}_2 + 100 \text{ ppm CO}$ was used in all the experiments of hydrogen oxidation. Methanol oxidation measurements were conducted in the same cell containing a 5-M $\text{CH}_3\text{OH} + 1.5\text{-M H}_2\text{SO}_4$ solution at 65 °C without H_2 gas back-feeding [14]. The electrode geometric area exposed to the electrolyte was 1 cm^2 . A large-area platinum flat electrode was used as a counter electrode and an Hg/HgSO_4 reference electrode was connected to the cell through a Luggin capillary. The potential values quoted are reported with respect to the normal hydrogen electrode (NHE). The electrochemical cell was connected to a Solartron mod. 1287 potentiostat/galvanostat and a Solartron mod. 1260 frequency response analyser, both interfaced with a GPIB card to a personal computer. EIS measurements were carried out in the frequency range 20 kHz–1 Hz at open circuit potential (OCP). The amplitude of the ac signal was always $10 \text{ mV}_{\text{pp}}$.

Full-cell electrochemical characterisation

Full-cell electrochemical tests were separately carried out on five different MEGAs (three with anode using the ENEA Pt–Ru/C catalyst and two with the E-Tek Pt–Ru/C catalyst) using a 106-cm^2 single cell incorporated in a Globe Tech Inc mod. 890 test station.

Cell voltage versus current density measurements were taken galvanostatically with a programmable power supply interfaced with a computer for data acquisition. To obtain a steady-state galvanostatic polarisation curve, the time for each measurement was found to be at least 0.5 min/point. Voltage was always measured directly onto copper thin sheets inserted between the end plates and graphite plates. The measurements were carried out using pure H_2 or $\text{H}_2 + 100 \text{ ppm CO}$ streams at cell temperature (T_{cell}) of 75 °C, with anode and cathode humidifying temperatures of 85 °C and 62 °C, respectively. For the cathode and anode, the gases flow rate is based on a H_2/O_2 stoichiometric ratio (S.R.) of 2.

Results and discussion

Table 1 summarises the solubility data of the ENEA and E-Tek samples in ethanol and methanol. With both solvents, the loss of ruthenium in the E-Tek catalyst at low and high temperatures was evident. In addition, this loss was clearly enhanced by ultrasonic treatment at 25 °C. In contrast, the ENEA catalyst showed higher stability in all the solubility tests.

Another difference between the two bimetallic catalysts is the presence of 2–3 wt.% sulfur in the E-Tek

Table 1 Solubilities of Pt–Ru/C catalysts in alcohols at different temperatures and times

| Solvent | Treatment | ENEA (wt.%) | E-Tek (wt.%) |
|----------|---------------------------|-------------|--------------|
| Ethanol | 25 °C–14 min ^a | <0.05 | 2.38 |
| Ethanol | 65 °C–60 min | 0.09 | 8.18 |
| Ethanol | 25 °C–11 days | ≤ 0.40 | 9.02 |
| Methanol | 25 °C–11 days | ≤ 0.40 | 10.47 |
| Methanol | 65 °C–60 min | 0.04 | 5.92 |

^aIn ultrasonic bath

catalyst, as evidenced by our XPS analysis not shown here and also from literature data [22, 23]. The presence of sulfur is mostly likely related to the E-Tek preparation method [24], similar to that of Watanabe et al. [8], which makes use of sodium bisulfite to convert the PtCl_6^{2-} precursor to a sulfite complex prior to the reduction to metallic platinum and ruthenium. In contrast, platinum and ruthenium in the ENEA catalyst are reduced simultaneously with only one reducing agent (NaBH_4) and a crystalline alloy is formed without sulfur impurity, as demonstrated by the XRD data presented in this work.

The anodic galvanostatic polarisation data of pure H_2 oxidation in 1-M H_2SO_4 solution at 25 °C are shown in Fig. 1. To compare the two catalysts, the electrolyte resistance (R_e) for each electrode was determined by means of EIS and the iR_e corrected data (obtained by subtracting the term $R_e i$ from the experimental E versus i plot) were reported. The ENEA and E-Tek Pt–Ru/C electrodes show the same performance characterised by a very low polarisation of activation and by the absence of diffusion limitation in the current range analysed.

Figure 2 shows the anode galvanostatic polarisation data of methanol oxidation at 65 °C. Also in this case, the electrolyte resistance (R_e) for each electrode was obtained by EIS and the iR_e corrected data were reported. The ENEA and E-Tek Pt–Ru/C electrodes show the same performance and at 150 mA cm^{-2} the electrode potential corrected for iR_e was in the range 430–435 mV versus NHE. Figure 3 illustrates the Bode plot of the ENEA and E-Tek catalysts at 65 °C and OCP. The difference between Z' (the real part of impedance) at 20 kHz and at 1 Hz represents the polarisation resistance R_p^o , which is the sum of all possible phenomena: charge transfer, diffusion and adsorption. The R_p^o is in the range $0.27\text{--}0.30 \Omega \text{ cm}^{-2}$, indicating the same methanol oxidation rate for the two catalysts.

EIS was also used to monitor and compare the degradation effects of carbon monoxide on the electrode performance at OCP [11, 20]. Bode plots registered continuously while the gas stream was changed from pure to poisoned H_2 (100 ppm of CO) furnished an ohmic resistance (R_e) that appears to be constant for both catalysts during contamination. The difference

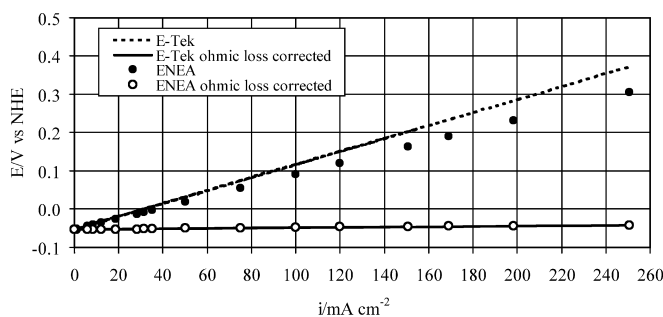


Fig. 1 Galvanostatic steady-state polarisation curves of H_2 oxidation of the ENEA and E-Tek Pt–Ru/C catalysts in 1 M H_2SO_4 solution at 25 °C. iR_e corrected polarisation data are also presented

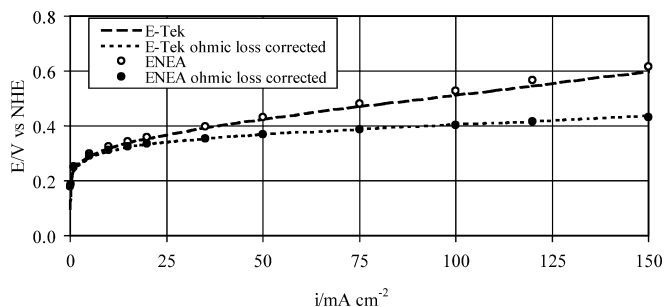


Fig. 2 Galvanostatic steady-state (250 s at each current) polarisation curves of methanol oxidation of the ENEA and E-Tek Pt–Ru/C catalysts in 5-M $\text{CH}_3\text{OH}/1.5\text{-M H}_2\text{SO}_4$ solution at 65 °C. iR_e corrected polarisation data are also presented

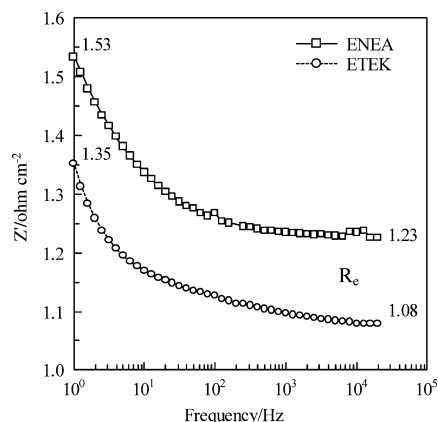


Fig. 3 Bode plots of the ENEA and E-Tek Pt–Ru/C gas diffusion electrodes at OCP versus NHE in 5-M $\text{CH}_3\text{OH}/1.5\text{-M H}_2\text{SO}_4$ solution at 65 °C

between Z' at low and high frequencies (R_p°), which can be ascribed to the hydrogen oxidation reaction in the catalytic sites, is strictly dependent on the active area. As carbon monoxide contaminates the Pt sites, the electrochemical active area decreases and the polarisation resistance increases rapidly. Figure 4 reports the trend of R_p° versus time of contamination for both catalysts and shows an increase from 30 $\text{m}\Omega \text{ cm}^{-2}$ to 1.10 $\Omega \text{ cm}^{-2}$ in only 80 min due to a reduction of the electrochemical area. At zero time, both catalysts have very low R_p° values, as already seen from the galvanostatic polarisation data (44 $\text{m}\Omega \text{ cm}^{-2}$).

Figure 5 shows the cell performance of MEGAs with different anode catalysts at 75 °C in H_2 and O_2 streams. As in the half-cell measurements, the performance is similar also at high current densities. Figure 6 presents the cell anode potential versus current density plots of the same MEGAs in $\text{H}_2 + 100 \text{ ppm CO}$ and O_2 streams. Within the error limit, the trend appears to be similar and at 350 mA cm^{-2} ; the overpotential was about 150 mV for both catalysts, showing the same results obtained with half-cell measurements in methanol. The electrochemical characterisation of the ENEA and E-Tek catalysts confirms that both samples have the

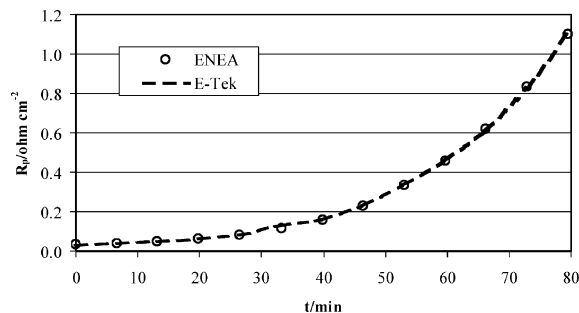


Fig. 4 Polarisation resistance at OCP versus time of the ENEA and E-Tek Pt–Ru/C gas diffusion electrodes in 1-M H_2SO_4 solution at 25 °C, under $\text{H}_2 + \text{CO}$ 100 ppm stream

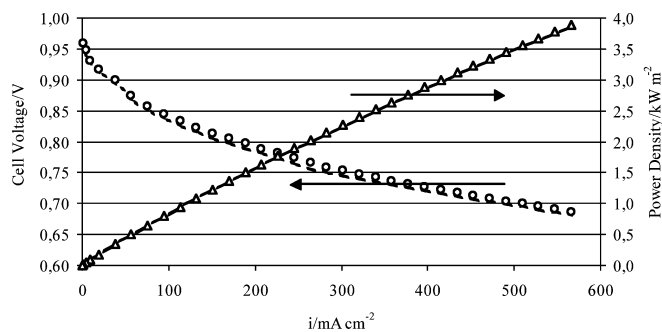


Fig. 5 Cell voltage and power density versus current density of MEGAs with the ENEA (\circ and Δ) and E-Tek (--- and —) Pt–Ru/C catalysts at the anode side, $T_{\text{cell}} = 75 \text{ °C}$ under H_2 and O_2 streams (1.4/1.4 abs. bar)

same behaviour in pure H_2 , in H_2 contaminated with CO and in methanol.

In a previous study [14], XRD patterns of the ENEA and E-Tek catalysts were registered, showing the face-centred cubic crystalline structure of Pt [25, 26]. Peaks deconvolution of XRD patterns were performed with both the Rietveld and X-Fit [27] programs to compute the lattice parameter, peak integrated intensity and peak width. The algebraic mean of the grain size (D) computed from the (111) and (220) diffraction peaks (the best resolved in the diffractograms) was $2.6 \pm 0.2 \text{ nm}$ for both catalysts.

Platinum and ruthenium form an fcc solid solution in the Pt-rich side of the composition range, i.e. $[\text{Ru}] < 60 \text{ at.}\%$ [28]. Since the atomic volume of Ru is 13.577 \AA^3 and that of Pt is 15.094 \AA^3 , the introduction of Ru in the Pt fcc structure reduces the lattice parameter a_{fcc} . According to the variation of a_{fcc} with composition for Pt–Ru bulk alloys [29, 30, 31], it is possible to obtain the atomic fraction of Ru present in the alloy. For the ENEA sample, we measured a value of $3.856 \pm 0.005 \text{ \AA}$ for the lattice parameter of the cubic phase, as determined by the peak profile fitting of the (220) reflection, corresponding to $54 \pm 5 \text{ at.}\%$ of Ru in the alloy according to literature data [28, 30]. For the E-Tek sample, a value of $3.883 \pm 0.005 \text{ \AA}$ was found, corresponding to $32 \pm 5 \text{ at.}\%$ of Ru in the solid solution

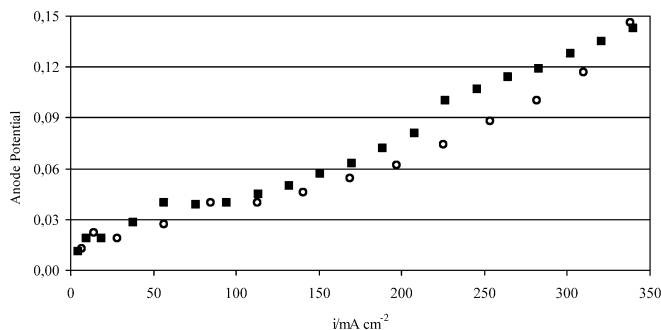


Fig. 6 Cell anode potential versus current density of MEGAs with the ENEA (○) and E-Tek (■) Pt-Ru/C catalysts, $T_{\text{cell}} = 75$ °C under $\text{H}_2 + \text{CO}$ 100 ppm and O_2 streams (1.4/1.4 abs. bar)

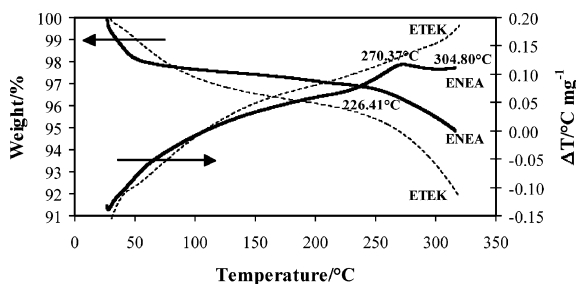


Fig. 7 TG scans of the ENEA and E-Tek Pt-Ru/C catalysts at 5 °C min^{-1} in air flow

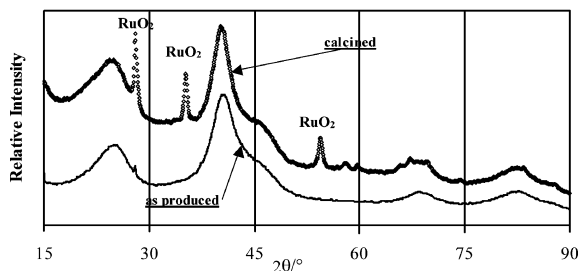


Fig. 8 XRD patterns of the ENEA Pt-Ru/C catalyst as-produced and after heat treatment at 270 °C for 1 h in air flow

[29, 31]. Several authors [21, 22, 24, 32, 33] have done similar XRD investigations on E-Tek catalysts. All these studies agree that the Ru metal content in this catalyst is significantly lower than the nominal Ru bulk content, implying that a significant amount of Ru is not included in the alloy (26.1–39.4 at.% of Ru in the solid solution), but present in an oxide phase. By comparing our results with the ones from the literature, we can suppose that part of the ruthenium in the E-Tek catalyst is outside the crystalline lattice of the alloy and not present in the Ru hcp crystalline structure, as seen by the absence of Ru peaks in XRD patterns. This Ru may instead form an amorphous ruthenium oxide. In agreement with this result, XPS measurements [20] revealed the presence of typical oxide and hydroxide bonds on the E-Tek catalyst. To evaluate the degree of crystalline phase in both samples, a fitting procedure was performed by the deconvolutions of carbon and alloy diffraction peaks and

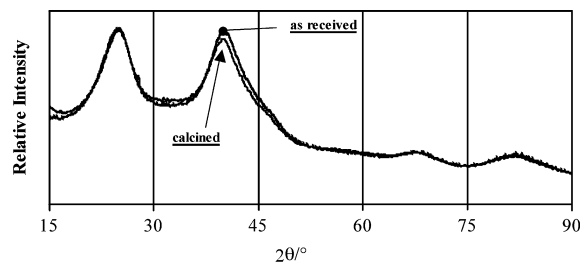


Fig. 9 XRD patterns of the E-Tek Pt-Ru/C catalyst as-received and after heat treatment at 270 °C for 1 h in air flow

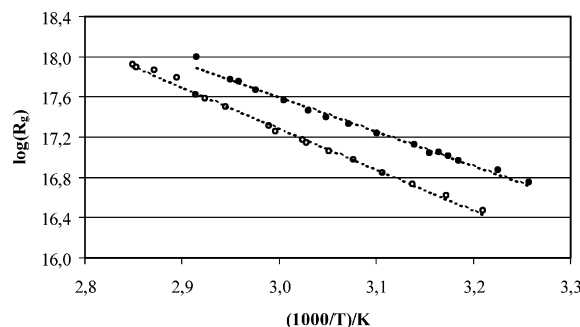


Fig. 10 $\log R_g$ versus $1/T \times 10^3$ of the ENEA (●) and E-Tek (○) Pt-Ru/C catalysts. R_g rates are expressed as molecules of CO converted to CO_2 per second per gram of metal

by measuring their integrated intensity, which is proportional to the crystalline fraction of the alloy. By comparing the intensity ratio of carbon and alloy diffraction peaks for both catalysts, it is possible to estimate the amount of alloy that crystallises. Since the (111) and (200) fcc reflections are not well resolved, we used the sum of their intensities for the computation of the quantity of crystalline phase. The integrated intensities of the carbon and (111) + (200) peaks of the ENEA and E-Tek catalysts [14] show an amount of crystalline alloy $40 \pm 3\%$ lower in the E-Tek sample with respect to the ENEA catalyst. This result confirms that part of metal in the E-Tek catalyst is not present as a crystalline phase and agrees with the low Ru content (at.%) present in the alloy with respect to the reported value [22, 24].

Figure 7 presents the TG of both catalysts in the range 25 – 300 °C in air flow. A weight decrease was observed for both catalysts mainly due to the combustion of carbon. We can exclude a predominant water desorption phenomenon because the weight loss was absent in nitrogen flow. A significant difference is the presence of an exothermic peak at approximately 270 °C in the ENEA catalyst. This peak is not present in the measurements carried out in nitrogen flow, most likely indicating an oxidative phenomenon. In addition, TG analyses not shown here of the pure Vulcan XC-72 carbon black or the ENEA Pt/C catalyst produced with the same process do not show this peak. Therefore, we can conclude that the oxidation of Ru occurs at this temperature. XRD data of the ENEA Pt-Ru/C calcined at 270 °C for 1 h in air (Fig. 8) supports this hypothesis

showing the presence of ruthenium oxide characteristic peaks at 2θ values of 28° , 35.2° and 54.4° [25]. In contrast, it was noticed that the behaviour of the E-Tek catalyst treated in the same manner (Fig. 9) is quite similar to that of the untreated sample. These results confirm that ruthenium in the ENEA catalyst is completely alloyed with platinum and part of it can be transformed to crystalline oxide by heating in air flow. This leads us to conclude that the ruthenium in the E-Tek sample cannot be oxidised by heat treatment because it is already present as amorphous oxide [22] or perhaps even as RuS unidentifiable by XRD.

The comparison of the steady-state catalytic activities (Fig. 10) follows the work of Bracchini et al. [19] showing that for the $\text{CO} + \text{O}_2$ reaction the ENEA Pt–Ru/C catalyst was significantly more active than the E-Tek Pt–Ru/C. The activation energy was somewhat lower for the ENEA Pt–Ru/C ($E_a = 16 \text{ kcal mol}^{-1}$) than the E-Tek Pt–Ru/C ($E_a = 19 \text{ kcal mol}^{-1}$). Thus, the results from catalytic activity reflect mostly the presence of differences in the chemical states of the catalysts that, together with XRD and TG characterisations, can explain their dissimilar chemical stabilities.

Conclusions

A new route for preparing high surface Pt–Ru/C catalysts at low temperature was defined. A satisfactory reduction process of the metals was achieved by means of a proprietary low temperature heat treatment. The performance of the prepared catalysts was similar to that of the commercial E-Tek sample, but with increased stability. The process has a lower cost than the traditional ones and appears to be easily scaled up to manufacturing levels.

The main characteristics of the process include:

- Metal precursors, reducing agents and carbon support are homogeneously and intimately mixed at room temperature in a highly stable single bath.
- A thermal treatment is provided up to 100°C ; thermal and concentration gradients are decreased in the suspension and small catalyst particles are obtained.

The catalyst produced is a real 50:50-at.% Pt–Ru alloy with much more crystalline phase with respect to commercial E-Tek sample. The electrochemical performances in hydrogen or methanol and the CO tolerance are similar to those of the E-Tek catalyst. In addition, the new catalyst is much more stable in ethanol and methanol even if heated or ultrasonicated.

Acknowledgements This work was supported by the Italian University and Scientific Research Ministry (MIUR). The authors thank Dr. M. Carewska (ENEA) for the TG analyses.

References

1. Oetjen HF, Schmidt VM, Stimming U, Trila F (1996) *J Electrochem Soc* 143:3838
2. Gasteiger A, Markovic N, Ross PN, Cairns EJ (1994) *J Phys Chem* 98:617
3. Gasteiger A, Markovic N, Ross PN (1995) *J Phys Chem* 99:16757
4. Lamy C, Lima A, Le Rhun V, Delime F, Coutanceau C, Leger JM (2002) *J Power Sources* 105:283
5. Luna AMC, Camara GA, Paganin VA, Ticianelli EA, Gonzalez ER (2000) *Electrochem Commun* 2:222
6. Bönemann H, Brinkmann R, Britz P, Endruschat U, Mörtel R, Paulus UA, Feldmeyer GJ, Schmidt TJ, Gasteiger HA, Behm RJ (2000) *J New Mater Electrochem Syst* 3:199
7. Schmidt TJ, Gasteiger HA, Behm RJ (1999) *Electrochem Commun* 1:1
8. Watanabe M, Uchida M, Motoo S (1987) *J Electroanal Chem* 229:395
9. Mukerjee S, Lee SJ, Ticianelli EA, McBreen J, Grgur BN, Markovic NM, Ross PN, Gialombardo JR, De Castro ES (1999) *Electrochem Solid State Lett* 2(1):12
10. Ioroi T, Fujiwara N, Siroma Z, Yasuda K, Miyazaki Y (2002) *Electrochem Commun* 4:442
11. Giorgi L, Antolini E, Pozio A, Passalacqua E (1998) *Electrochim Acta* 43:3675
12. Okada T, Ayato Y, Yuasa M, Sekine I (1999) *J Phys Chem B* 103:3315
13. Okada T, Ayato Y, Satou H, Yuasa M, Sekine I (2001) *J Phys Chem B* 105:6980
14. Pozio A, Silva RF, De Francesco M, Cardellini F, Giorgi L (2003) *Electrochim Acta* 48:1627
15. Pozio A, De Francesco M, Cemmi A, Cardellini F, Giorgi L (2002) *J Power Sources* 105:13
16. Pozio A, Giorgi L, De Francesco M, Silva RF, Lo Presti R, Danzi A (2002) *J Power Sources* 112:491
17. Ayres G, Young F (1951) *Anal Chem* 23:299
18. Ayres G, Young F (1950) *Anal Chem* 22/10:1277
19. Bracchini C, Indovina V, De Rossi S, Giorgi L (2000) *Catal Today* 55:45
20. Giorgi L, Pozio A, Bracchini C, Giorgi R, Turtù S (2001) *J Appl Electrochem* 31:325
21. Rolison DR, Hagans PL, Swider KE, Long JW (1999) *Langmuir* 15:774
22. Aricò AS, Creti P, Modica E, Manforte G, Baglio V, Antonucci V (2000) *Electrochim Acta* 45:4319
23. Radmilovic V, Gasteiger HA, Ross Jr PN (1995) *J Catal* 154:98
24. Lasch K, Hayn G, Jorissen L, Garche J, Besenhardt O (2002) *J Power Sources* 105:305
25. Chunzi H, Kunz HR, Fenton JM (1997) *J Electrochem Soc* 144:970
26. Coelho AA, Cheary RW (1996) X-ray line profile fitting program. School of Physical Sciences, University of Technology, Sydney, Australia
27. Massalski TB (1986) Binary alloy phase diagrams, vol 2. American Society for Metals
28. Lalonde G, Denis MC, Dodelet JP, Schulz R (1999) *J Alloys Compd* 292:301
29. Pearson WB (1956) Handbook of lattice spacing and structures of metals and alloys. Pergamon, London
30. Gasteiger HA, Ross Jr PN, Cairns EJ (1993) *Surf Sci* 293:67
31. Martelli S, Di Nunzio PE (2001) Proceedings from the 6th Italian Meeting on Nanophase Materials, Rome, Italy
32. Mukerjee S, Urian RC (2002) *Electrochim Acta* 47:3219
33. Shukla AK, Aricò AS, El-Khatib KM, Kim H, Antonucci PL, Antonucci V (1999) *Appl Surf Sci* 137:20